

# Molecular design of coumarin dyes with high efficiency in dye-sensitized solar cells

Xiao Zhang<sup>a,b</sup>, Jing-Jun Zhang<sup>a</sup>, Yong-Yao Xia<sup>a,\*</sup>

<sup>a</sup> Chemistry Department and Shanghai Key Laboratory of Molecular Catalysis and Innovative Materials, Fudan University, Shanghai 200433, China

<sup>b</sup> College of Chemistry and Molecular Engineer, Qingdao University of Science & Technology, Qingdao 266042, China

Received 31 March 2007; received in revised form 24 July 2007; accepted 2 August 2007

Available online 7 August 2007

## Abstract

Density functional theory (DFT) and time-dependent DFT calculation have been applied to study the coumarin dyes which act as photosensitizer in dye-sensitized solar cells. The absorption spectra of coumarin dyes in ethanol can be well reproduced with theoretical method. The outstanding performance of NKX-2311 roots in higher light harvesting efficiency and more efficient electron injection efficiency into conduction band of TiO<sub>2</sub> electrode according to our computation. Absorption peaks and HOMO energy levels of dyes can be employed as the two effective theoretical parameters for the judgement of their solar to energy efficiency. New coumarin dyes which probably possess higher efficiency were designed referring to our conclusions.

© 2007 Elsevier B.V. All rights reserved.

**Keywords:** Density functional theory; Dye-sensitized solar cell; Coumarin dyes

## 1. Introduction

Dye-sensitized solar cells (DSC) have been attracting considerable attention owing to their comparatively low cost and high efficiency in recent years [1–3]. Dyes are the crucial factor for the solar to energy efficiency of DSCs. There are several types of properties related with dyes which determine the efficiency of DSCs, such as sunlight harvesting efficiency and quantum yield of electron injection on the surface of semiconductor film, etc. [4].

Polybipyridyl ruthenium dyes are the most efficient photosensitizer in DSCs by now [5]. Molecular modification of these dyes is a tough task for their complicated synthesis routes; moreover, the raw materials such as noble metals applied in the synthesis procedures are rather expensive. Organic dyes have also been applied as photosensitizers in DSCs [6–8]. Organic dyes have several advantages over ruthenium complexes: the cost of organic dyes is much lower than ruthenium complexes; moreover, molecular design of organic dyes is more convenient than

that of ruthenium complexes for variability of their molecular structures.

Coumarin dyes are among organic dyes which possess high solar to energy transfer efficiency in DSCs [9–12]. Numerous experimental methods have been applied to acquire novel organic coumarin dyes with higher efficiency. Although experimental molecular modification is a powerful and straightforward route to get new dyes, the synthesis process is not only expensive but time-consuming. Theoretical calculation method is another powerful tool for molecular design, and conclusions drawn from calculation are valuable guideline for synthesis of new efficient dyes. Theoretical investigation has been carried out on polybipyridyl ruthenium dyes [13–15]. Only very recently, theoretical methods have been employed to investigate absorption spectra of coumarin dyes [16]. Up to now, no theoretical methods have been applied to study the structure–activity relationship (SAR) of coumarin dyes about their application in dye-sensitized solar cells.

In the present work, density functional theory (DFT) method has been applied to elucidate the SAR for a series of coumarin dyes (NKX-2398, NKX-2388, NKX-2311, NKX-2586, shown in Fig. 1). They are named according to the researcher who synthesized the dyes [4]. Their bone structures are the same as

\* Corresponding author. Tel.: +86 21 55664177; fax: +86 21 55664177.  
E-mail address: [yyxia@fudan.edu.cn](mailto:yyxia@fudan.edu.cn) (Y.-Y. Xia).



Table 1

The absorption peaks of computational and experimental data of the four coumarin dyes (in nm) and their solar to energy efficiency in the experiments of Hara et al. [4]

	$\lambda_{\max}$ (experiment) [4]	$\lambda_{\max}$ (computation)	$\eta$ (%) [4]
NKX-2398	451	422	3.4
NKX-2388	493	459	4.1
NKX-2311	504	506	5.2
NKX-2586	506	552	3.5

From NKX-2388, NKX-2311 to NKX-2586, the conjugated structures become larger although their substituent groups connected to the end of methine moiety are the same. It is indicated that the absorption spectra of dyes red-shifted with size expansion of their conjugate systems according to our calculation. On the other side, the character of the substituent groups plays an important part in the UV–vis absorption property of these dyes. The substituent group which acts as strong electron acceptor group, such as cyano group, is advantageous to the red-shift of absorption spectra. As a whole, the UV–vis absorption spectra of these coumarin dyes can be well reproduced with the theoretical method.

It is well known that red shift in the absorption spectra of dyes are desirable for harvesting the sunlight when they are employed as the photosensitizer in dye-sensitized solar cells. From NKX-2398, NKX-2388 to NKX-2311, the absorption bands shift to longer wavelength, which means the dye NKX-2311 can make better use of sunlight. It is probably the reason why NKX-2311 displays higher efficiency than the other two dyes. The light harvesting efficiency of NKX-2586 is more efficient than NKX-2311, while the cell efficiency of NKX-2586 is much lower than that of NKX-2311 referring to the experiment. It is due to that light harvesting efficiency of the photosensitizer is not the exclusive factor to determine the efficiency of solar cells. We will elucidate the cause of this phenomenon in the following part of our article.

The molecular orbitals involved in the analysed transitions were examined with DFT method. The electronic structures of these dyes are quite similar although their sizes of conjugated systems and substituted groups are distinct from each other. The HOMO and LUMO orbital of NKX-2311 are depicted in Fig. 3 as the representation. It can be easily identified that the absorption bands of these four dyes are attributed to  $\pi \rightarrow \pi^*$  transition. There is one distinct phenomenon which cannot be ignored: the LUMO orbital possesses larger composition of carboxyl group located at the end of methine unit chain ( $-\text{CH}=\text{CH}-$ ) compared

with the HOMO orbital which is liable to located at ring moieties. The conclusion can be drawn that electron transfer from the ring moieties towards carboxyl groups takes place during the excitation process of the dyes. Because the dyes are anchored onto the surface of semiconductor surface through carboxyl group, electron injection process will be facilitated as the dyes are excited. The electronic structures of these coumarin dyes are in favor of the high overall efficiency of the solar cells.

### 3.2. The driving force for electron injection of the dyes

Electron transfer process across the surface of semiconductor film becomes the crucial factor after the dyes are oxidized. The electron injection process involves electron transfer from discrete excited states of dyes to a continuum of electronic levels in the semiconductor, so the total electron transfer rate can be demonstrated as [20,21]:

$$k_{\text{et}} = \frac{2\pi}{\hbar} \int_0^\infty dE \rho(E) |\bar{H}(E)|^2 \frac{1}{\sqrt{4\pi\lambda k_B T}} \times \exp\left(-\frac{(\Delta G^\circ + \lambda - E)^2}{4\lambda k_B T}\right) \quad (1)$$

In this equation,  $\bar{H}(E)$  is the average electronic coupling between the excited states of dyes and the accepting states in the semiconductor.  $\rho(E)$  denotes the density of accepting states at energy  $E$  relative to the conduction band edge.  $\Delta G^\circ$  is the energy gap between the oxidation potential of excited state dyes and the conduction band edge of semiconductor  $E_{\text{cb}} - E_{\text{dye}}$ . As has been analyzed in our previous research [22], the rate of electron transfer of the dye molecules with similar molecular structures mainly depends on the energy gap between the oxidation potential of excited-state dyes and the conduction band edge of semiconductor  $E_{\text{cb}} - E_{\text{dye}}$ . The  $E_{\text{cb}} - E_{\text{dye}}$  value is denoted as the driving force of the electron injection, and larger driving force are desirable for more rapid electron injection rate and then higher overall efficiency of DSCs.

The energy levels of the excited state of the four dyes are demonstrated in Fig. 4 consulting the absorption peaks of the simulated UV–vis spectra. The energy levels of their singlet excited state  $S_1$  shift to be positive from NKX-2398, NKX-2388, NKX-2311 to NKX-2586. The energy gaps between the conduction band of  $\text{TiO}_2$  and  $S_1$  state are 1.24, 0.85, 0.67, and 0.60 eV for these four dyes, respectively. Their driving force for electron injection decreases in this order. According to Eq. (1), the order of electron injection rate is  $\text{NKX-2398} > \text{NKX-}$

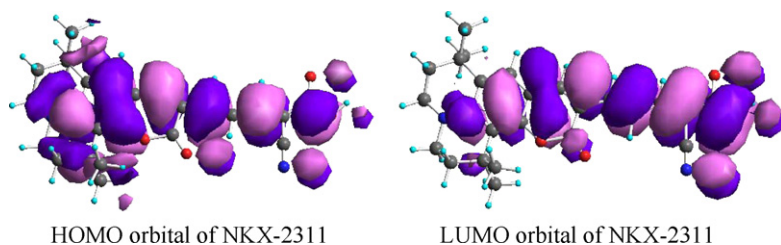


Fig. 3. The structures of frontier orbitals for NKX-2311.

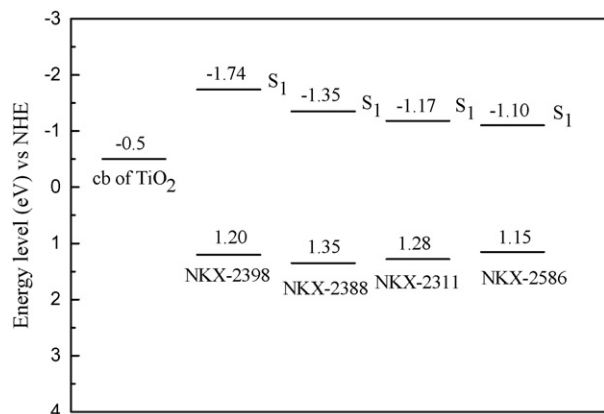


Fig. 4. Energy level diagram of conduction bands of  $\text{TiO}_2$ , ground state and singlet excited states of coumarin dyes.  $S_1$  denotes the first singlet excited states of dyes.

2388 > NKX-2311 > NKX-2586. The electron injection process of NKX-2311 is more liable to take place than that of NKX-2586. It is probably the reason why the overall efficiency of solar cells with NKX-2586 is much lower than that with NKX-2311 although the light harvesting efficiency of NKX-2586 exceeds that of NKX-2311. To summarize, NKX-2311 possesses not only broad absorption band in higher wavelength region but also favorable energy level for its singlet excited state. Both of these two factors are advantageous to its solar to energy efficiency.

### 3.3. Theoretical parameters to judge electrochemical performance of coumarin dyes

The location of absorption band and energy level of singlet excited state can be applied as the criteria to judge the electrochemical performance of coumarin dyes. The UV–vis absorption spectra can be well reproduced with theoretical method, but the value of oxidation potential is essential to calculation of  $S_1$  energy level. The simulation of oxidation potential is beyond the capacity of our calculation. Fortunately, we found the oxidation potential correlates with energy level of HOMO orbital. As is demonstrated in Fig. 5, the energy level of HOMO

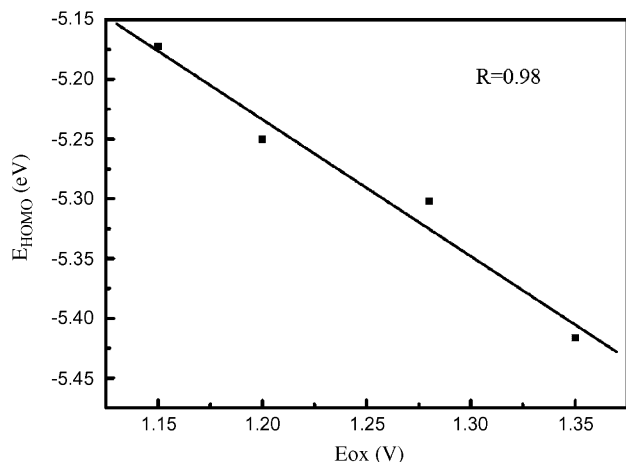


Fig. 5. The linear relation between oxidation potential values and energy levels of HOMO orbitals.

orbital is linear with the oxidation potential measured with experimental methods [4] for this series of coumarin dyes. More positive HOMO energy level will inevitably make the oxidation potential negative. Less positive oxidation potential results in more favorable excited state energy level for electron injection consulting the distribution of energy levels in Fig. 4 and the relationship between the HOMO energy level and Eox in Fig. 5. In summary, dyes with absorption bands in higher wavelength region and more positive HOMO energy level compared with NKX-2311 is more liable to display better electrochemical performance than NKX-2311.

UV–vis absorption spectrum and HOMO energy level can be simulated conveniently with theoretical method. Although the calculated results cannot provide quantitative data about the performance of dyes, the theoretical method may act as a convenient and low-cost tool for selection and molecular design of new coumarin dyes with higher efficiency.

### 3.4. Molecular design of new coumarin dyes based on NKX-2311

One approach to improve the performance of coumarin dyes is to expand the methine unit of NKX-2311. The expansion of conjugated structures will result in red shift of their absorption bands, but it makes the synthesis procedure more complicated and longer methine chain is liable to cause aggregation of dyes which is disadvantage for the efficiency of these dyes [23].

We tried to design dyes with better efficiency based on NKX-2311. The molecular modification route is to introduce substituent groups on the molecular bone of NKX-2311. Substituent groups with different electron character and steric hindrance property were introduced into different substitution sites of NKX-2311. The substitution sites are numbered in Fig. 6. The substituents applied can be divided into three types: electron-donating substituents ( $-\text{OH}$ ,  $-\text{NH}_2$ ,  $-\text{OCH}_3$ ), electron-withdrawing substituents ( $-\text{CF}_3$ ,  $-\text{F}$ ,  $-\text{CN}$ ) and two substituents with steric effect (shown in Table 2). These substituents were located at site a, b, c, d, e, respectively. Thirty-six model molecules with different substituents at the vacant sites were analyzed with DFT method in order to screen out new dyes with potential.

Their absorption peaks and energy levels of HOMO orbital simulated with theoretical method are summarized in Table 2. The absorption band peak and HOMO orbital energy level of NKX-2311 were confirmed to be 505 nm and

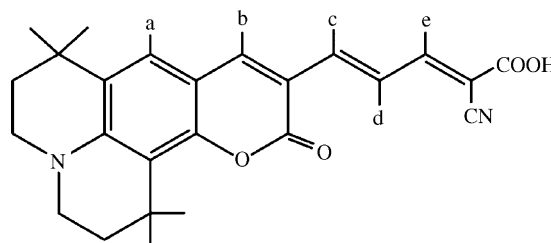
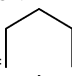
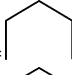
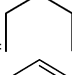
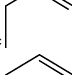
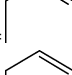
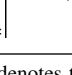


Fig. 6. The substitution sites on NKX-2311.

Table 2

The absorption peaks (in nm) and energy levels of HOMO orbitals (in eV) for the model molecules simulated with DFT method

Substituent group	$\lambda_{\max}$ (nm)	Evaluation <sup>a</sup>	$E_{\text{HOMO}}$ (eV)	Evaluation <sup>a</sup>
a=–OH	505	Y	–5.3010	N
a=–NH <sub>2</sub>	510	Y	–5.2142	Y
a=–OCH <sub>3</sub> <sup>b</sup>				
a=–CF <sub>3</sub>	510	Y	–5.3846	N
a=–F	497	N	–5.3947	N
a=–CN	510	Y	–5.5168	N
b=–OH	493	N	–5.3231	N
b=–NH <sub>2</sub>	485	N	–5.2800	Y
b=–OCH <sub>3</sub>	505	Y	–5.3283	N
b=–CF <sub>3</sub>	543	Y	–5.4172	N
b=–F	495	N	–5.3957	N
b=–CN	568	Y	–5.4779	N
c=–OH	495	N	–5.3231	N
c=–NH <sub>2</sub>	481	N	–5.2679	Y
c=–OCH <sub>3</sub>	510	Y	–5.3141	N
c=–CF <sub>3</sub>	574	Y	–5.3438	N
c=–F	505	Y	–5.3770	N
c=–CN	585	Y	–5.4289	N
d=–OH	543	Y	–5.1623	Y
d=–NH <sub>2</sub>	559	Y	–4.9527	Y
d=–OCH <sub>3</sub>	529	Y	–5.1884	Y
d=–CF <sub>3</sub>	523	Y	–5.3707	N
d=–F	532	Y	–5.2700	Y
d=–CN	524	Y	–5.4578	N
e=–OH	485	N	–5.2991	Y
e=–NH <sub>2</sub>	459	N	–5.2396	Y
e=–OCH <sub>3</sub>	490	N	–5.2741	Y
e=–CF <sub>3</sub>	549	Y	–5.3092	N
e=–F	503	N	–5.3435	N
e=–CN	602	Y	–5.4031	N
a, b= 	529	Y	–5.2461	Y
b, c= 	513	Y	–5.2586	Y
c, d= 	505	Y	–5.2349	Y
a, b= 	513	Y	–5.2287	Y
b, c= 	544	Y	–5.2787	Y
c, d= 	526	Y	–5.2496	Y

“Y” denotes that this property of this model dye is superior to that of NKX-2311 and “N” denotes that this property of this model dye is inferior to that of NKX-2311.

<sup>a</sup> The evaluation means the relative performance of the model dyes compared with that of NKX-2311.

<sup>b</sup> The geometry optimization of model molecule with methoxy group at site ‘a’ failed in our computation.

–5.3020 eV by means of theoretical method, which means that coumarin dyes with absorption peak at wavelength higher than 505 nm and HOMO energy level situated to be positive than –5.3020 eV are promising dyes with higher efficiency.

As is depicted in Table 2, electronic effects of the substituents affect the performance of the model dyes greatly. As

a whole, the attachment of electron-withdrawing substituents is more liable to induce red shift of the absorption spectra, while electron-donating substituents are likely to result in positive shift of HOMO energy level. It seems that it is a great task to pick out one substituent which can meet the two requirements. Fortunately substitution at site ‘d’ always causes red shift of absorption spectra no matter what kind of substituent is introduced. Model dyes with electron-donating substituents at site ‘d’ are promising photosensitizers in dye-sensitized solar cells.

Two kinds of substituents with steric effect (shown in Table 2) are also located at spare sites of NKX-2311. Two parameters of the six dyes are also calculated by means of theoretical method. It is surprising that all of these dyes meet these two requirements, which means substituent with steric effect is favorable for higher performance of dyes. On the other hand, their steric effect can prevent the dyes from aggregation efficiently as they are absorbed onto the surface of semiconductor film. To summarize, introduction of electron-donating substituents at site ‘d’ and the two kinds of substituents with steric effect are effective methods to get new promising coumarin dyes. This conclusion is a valuable clue for molecular modification of coumarin dyes.

#### 4. Conclusions

DFT method has been employed to examine the light harvesting and electron injection process from excited-state coumarin dyes into conduction band of semiconductor electrode. The simulated UV–vis absorption peaks of coumarin dyes fit well with the experimental data. According to our computational results, the expanding of conjugated system always results in red shift of absorption band. The absorption band of NKX-2398 and NKX-2388 are situated in shorter wavelength region compared with that of NKX-2311, which means the light harvesting efficiency of NKX-2311 is higher than the other two dyes. That is the reason why the overall efficiency of these two dyes is lower than NKX-2311.

Energy gaps between the conduction band edge of TiO<sub>2</sub> and excited-state oxidation potential of dyes can be employed as the driving force for electron injection. Our computation indicated that the driving force of NKX-2311 is larger than that of NKX-2586. The predominant performance of NKX-2311 roots in its high light harvesting efficiency and favorable excited state energy level.

As HOMO energy level is linear with oxidation potential, simulated absorption spectrum and HOMO orbital energy level can be employed to judge the efficiency of the dyes. These two parameters can be obtained with theoretical method, and then the efficiency of coumarin dyes can be figured out before they are synthesized. By means of this method, it is found out that electron-donating substituents at site ‘d’ and two kinds of substituents with steric effect are favorable for the efficiency of coumarin dyes. Our computational method is proved to be a powerful tool for molecular modification of coumarin dyes which will save us much time and money.



## Acknowledgements

This work was partially supported by the National Natural Science Foundation of China (No. 20633040) and the program of New Century Excellent Talents in University of China (2005). All the calculations have been performed at the Fudan High-end Computing Center.

## References

- [1] M. Grätzel, *J. Photochem. Photobiol. A: Chem.* 164 (2004) 3–14.
- [2] B. O' Regan, M. Grätzel, *Nature* 353 (1991) 737–740.
- [3] M. Grätzel, *Nature* 414 (2001) 338–344.
- [4] K. Hara, T. sato, R. Katoh, A. Furube, Y. Ohga, A. Shinpo, S. Suga, K. Sayama, H. Sugihara, H. Arakawa, *J. Phys. Chem. B* 107 (2003) 597–606.
- [5] M.K. Nazeeruddin, A. Kay, I. Rodicio, R. Humphry-Baker, E. Müller, P. Liska, N. Vlachopoulos, M. Grätzel, *J. Am. Chem. Soc.* 115 (1993) 6382–6390.
- [6] K. Hara, M. Kurashige, S. Ito, A. Shinpo, S. Suga, K. Sayama, H. Arakawa, *Chem. Commun.* (2003) 252–253.
- [7] S.L. Li, K.J. Jiang, K.F. Shao, L.M. Yang, *Chem. Commun.* (2006) 2792–2794.
- [8] D.P. Hagberg, T. Edvinsson, T. Marinado, G. Boschloo, A. Hagfeldt, L.C. Sun, *Chem. Commun.* (2006) 2245–2247.
- [9] K. Hara, T. sato, R. Katoh, A. Furube, T. Yoshihara, M. Murai, M. Kurashige, S. Ito, A. Shinpo, S. Suga, H. Arakawa, *Adv. Funct. Mater.* 15 (2005) 246–252.
- [10] K. Hara, M. Kurashige, Y. Dan-oh, C. Kasada, A. Shinpo, S. Suga, K. Sayama, H. Arakawa, *New J. Chem.* 27 (2003) 783–785.
- [11] K. Hara, Y. Tachibana, Y. Ohga, A. shinpo, S. Suga, K. Sayama, H. Sugihara, H. Arakawa, *Sol. Energy Mater. Sol. Cells* 77 (2003) 89–103.
- [12] R. Katoh, A. Furube, K. Hara, S. Murata, H. Sugihara, H. Arakawa, M. Tachiya, *J. Phys. Chem. B* 106 (2002) 12957–12964.
- [13] J.F. Guillemoles, V. Barone, L. Joubert, C. Adamo, *J. Phys. Chem. A* 106 (2002) 11354–11360.
- [14] M.K. Nazeeruddin, F. De Angelis, S. Fantacci, A. Selloni, G. Viscardi, P. Liska, S. Ito, B. Takeru, M. Grätzel, *J. Am. Chem. Soc.* 127 (2005) 16835–16847.
- [15] F. De Angelis, S. Fantacci, A. Selloni, M.K. Nazeeruddin, *Chem. Phys. Lett.* 415 (2005) 115–120.
- [16] Y. Kurashige, T. Nakajima, S. Kurashige, K. Hirao, Y. Nishikitani, *J. Phys. Chem. A* 111 (2007) 5544–5548.
- [17] V. Barone, M. Cossi, *J. Phys. Chem. A* 102 (1998) 1995–2001.
- [18] M. Cossi, V. Barone, R. Cammi, J. Tomasi, *Chem. Phys. Lett.* 255 (1996) 327–335.
- [19] M.J. Frisch, et al., *Gaussian 03, Revision C.02*, Gaussian Inc, Wallingford, CT, 2004.
- [20] J.B. Asbury, E. Hao, Y. Wang, H.N. Ghosh, T. Lian, *J. Phys. Chem. B* 105 (2001) 4545–4557.
- [21] N.A. Anderson, T. Lian, *Coord. Chem. Rev.* 248 (2004) 1231–1248.
- [22] X. Zhang, J.J. Zhang, Y.Y. Xia, *J. Photochem. Photobiol. A: Chem.* 185 (2007) 283–288.
- [23] Z.S. Wang, K. Hara, Y. Dan-oh, C. Kasada, A. Shinpo, S. Suga, H. Arakawa, H. Sugihara, *J. Phys. Chem. B* 109 (2005) 3907–3914.